Neuron, Volume *79*

Supplemental Information

A Conformational Intermediate in Glutamate Receptor Activation

Albert Y. Lau, Héctor Salazar, Lydia Blachowicz, Valentina Ghisi, Andrew J.R. Plested, and Benoît Roux

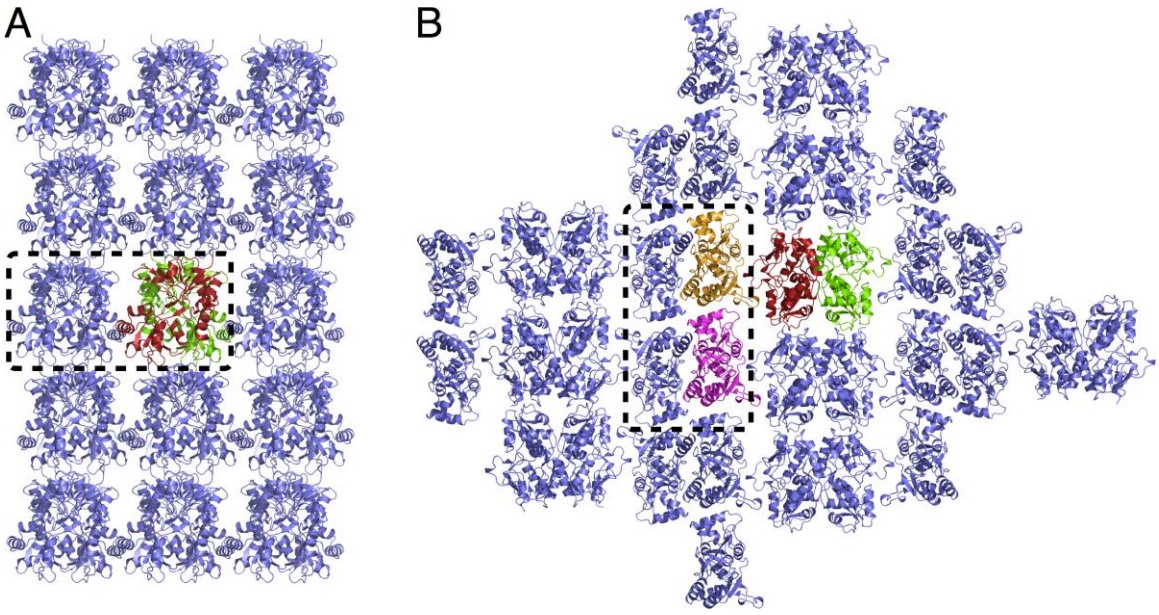

Figure S1. Crystal packing of GluA2-L483Y-A665C in the $P2_12_12$ space group, related to Figure 1. (**A**) The view perpendicular to the a–b plane. Only a layer containing Mol1 (brown), Mol2 (green), and molecules related by crystallographic symmetry (blue) is shown. A Mol1–Mol2 tetramer is boxed. (**B**) The view perpendicular to the b–c plane. All molecules within the asymmetric unit – Mol1, Mol2, Mol3 (orange), and Mol4 (magenta) – are shown. A Mol3–Mol4 tetramer is boxed.

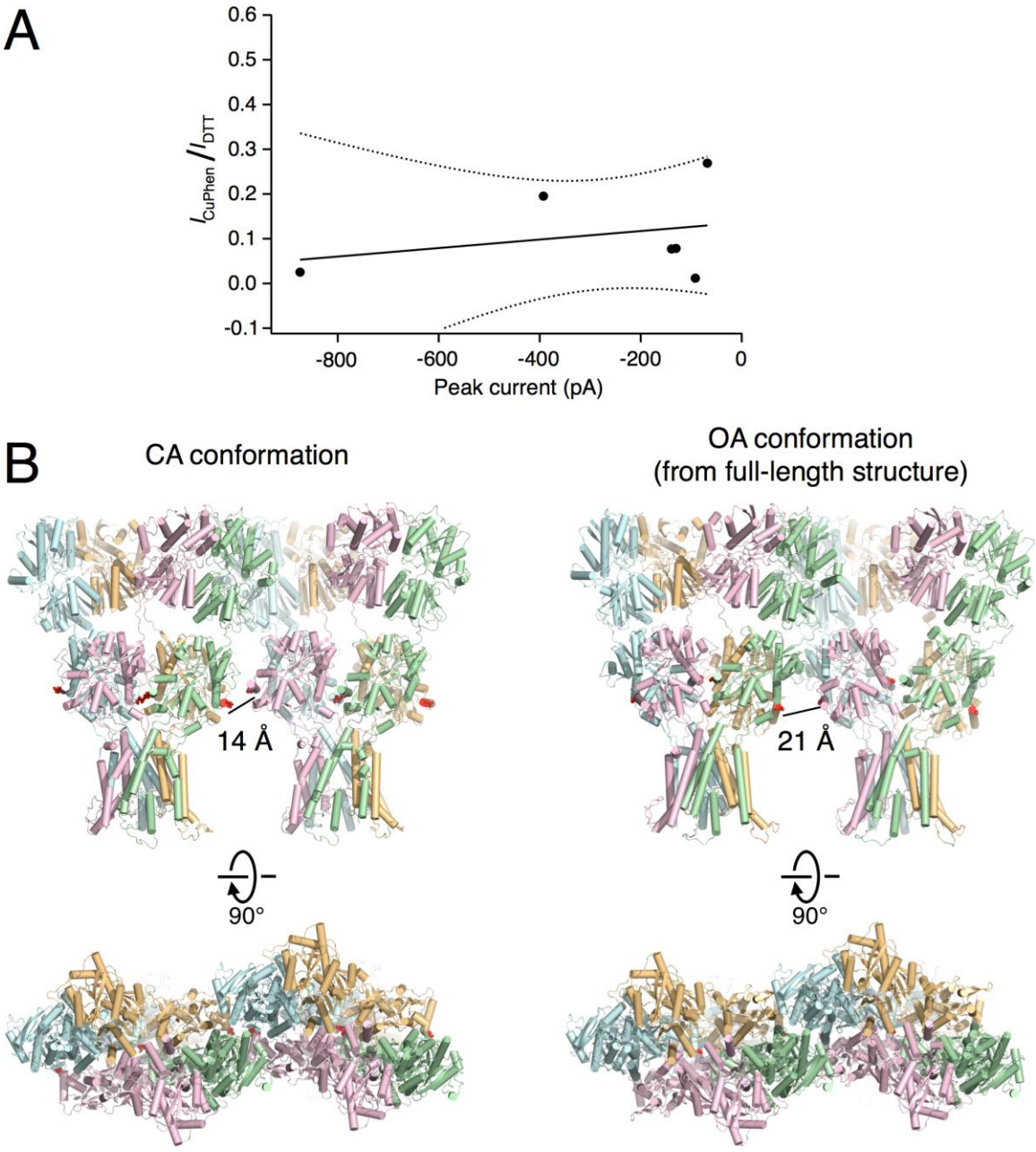

Figure S2. The GluA2 A665C mutation is unlikely to lead to crosslinks between receptors, related to Figure 2. (**A**) Inhibition of GluA2-A665C by CuPhen is unrelated to channel density (inferred from the peak current). A linear regression yields R^2 = 0.09; the dotted lines show the 95% confidence interval for the fit. (**B**) Modeling the LBDs in the closed-angle (CA) conformation (left) into the LBD layer of the full-length GluA2 structure (Sobolevsky et al., 2009) does not allow the surface-exposed cysteines at position 665 (red spheres) to approach closer than 14 Å (Cα–Cα

distance) due to steric hindrance from the ATD. Subunits A, B, C, and D are colored green, pink, blue, and yellow, respectively. The ATD, LBD, and TMD layers were each treated separately as rigid bodies. Similar modeling performed for the full-length GluA2 structure in the open angle (OA) conformation (right) indicates that the Cα atoms at position 665 cannot approach closer than 21 Å, again due to steric hindrance from the ATD. The modeling suggests that regardless of whether the LBDs are in the CA or OA conformation, disulfide bond formation between receptors at residue 665 is prohibited.

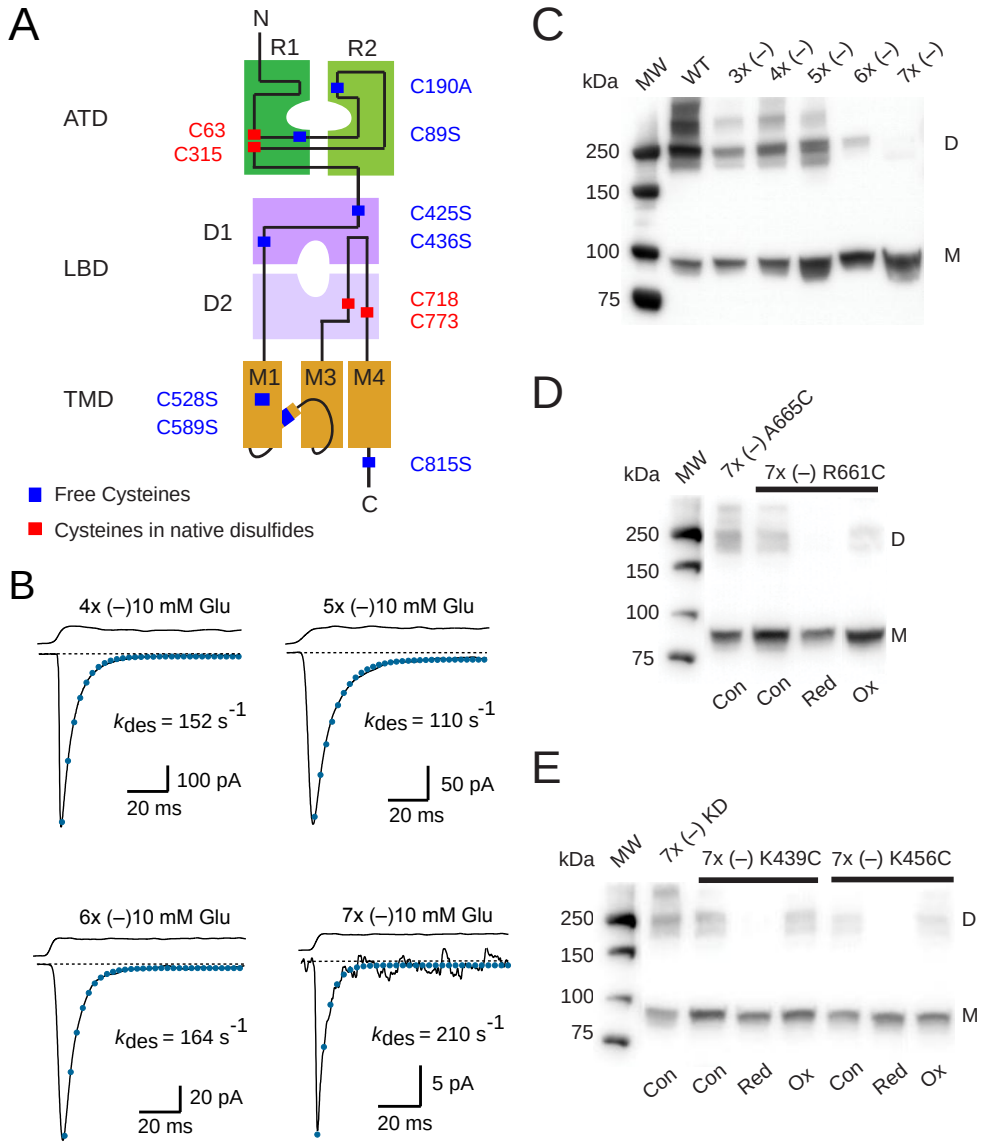

Figure S3. Construction of receptors without free cysteines, related to Figure 3. (**A**) Topology diagram for the GluA2 receptor showing the amino-terminal domain (ATD), the ligand-binding domain (LBD), the transmembrane domain (TMD), and the carboxyl-terminal tail. The cysteines that were replaced by serine or alanine are illustrated as blue squares. The four cysteines that are already making disulfide bonds are indicated by red squares. (**B**) The 4x (–), 5x (–), 6x (–) and 7x (–) constructs show similar activation and desensitization properties to wild type, but with a decrease in the level of current expressed with each subsequent cysteine substitution. (**C**) Western blot analysis of spontaneous oligomerization of GluA2

mutants in oxidizing conditions. From left to right: wild-type GluA2, the C190A-C436S-C528S triple mutant (3x Cys (–)), and additional cysteine substitutions as follows: C815S (4x Cys (–)), C589S (5x Cys (–)), C89S (6x Cys (–)), and C425S (7x Cys (–)). 7x Cys (–) ran ~90% as a monomer. (**D**) Western blot showing that the mutant R661C displays weaker dimer formation in oxidizing conditions compared with A665C. (**E**) Western blot showing that dimer formation for single mutants inserted on the 7x (–) background is weaker than for the double mutant K439C-D456C.

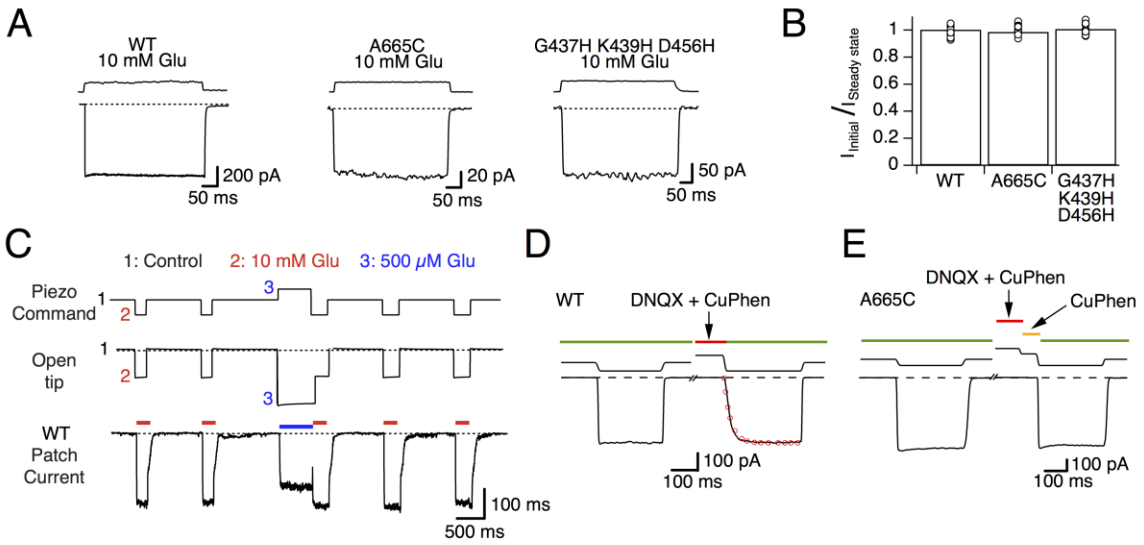

Figure S4. Conditions and protocols used to study state-dependent crosslinking, related to Figure 5. (**A**) Block of desensitization by cyclothiaziade (CTZ, 100 µM) for wild-type GluA2, the A665C mutant, and the G437H-K439H-D456H mutant. Responses were activated by 10 mM glutamate. The fast rise time, coupled with minimal sag after the peak, suggests desensitization was almost entirely absent. (**B**) In CTZ, the ratio of peak to steady-state current was 100 ± 1% for wild type, 98 ± 1% for A665C, and 100 ± 2% for G437H-K439H-D456H (*n* = 14 in each case). (**C**) The upper traces show the piezo command voltage, transitioning between three barrels. The middle traces are junction potentials at the open tip of the patch pipette. The lower trace shows wild-type GluA2 responses to pulses of 10 mM glutamate (red bars) flanking an application of 500 µM (blue bars). (**D**) Measurement of DNQX unbinding rate and trapping in the antagonist-bound state. Test responses to 10 mM glutamate in 5 mM DTT and 100 µM CTZ (green bars) were compared before and after application of 10 µM DNQX, 100 µM CTZ, and 10 µM CuPhen (red bars). After the application of antagonist, the relaxation of the current is dominated by unbinding of the antagonist (single exponential fit, red open circles, τ = 20 ms; *n* = 5). (**E**) 10 μM CuPhen and 100 µM CTZ were applied in the absence of DNQX for 40 ms to allow the release of the antagonist, while maintaining trapping. Immediately, a test pulse was applied to measure the amount of trapping. In this trace, the entire

application of CuPhen was 1.04 s (breaks are 900 ms). Notably, the test pulse after trapping is indistinguishable from that before trapping.

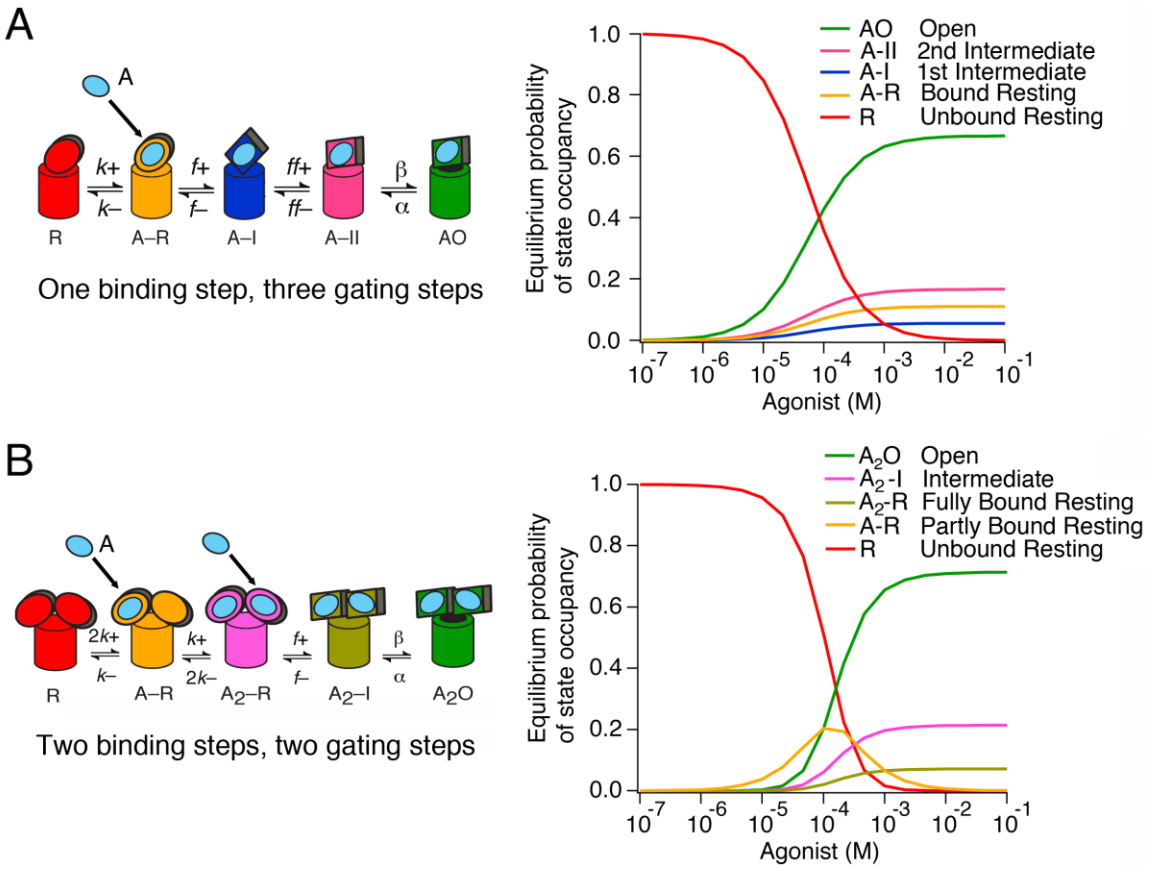

Figure S5. At equilibrium, log-normal inhibition with concentration corresponds to trapping in partially glutamate-bound states, related to Figure 5. Briefly, a *Q*-matrix of the mechanism was constructed for each given concentration, *Q*(c), using typical rate constants for glutamate receptors. The state occupancy vector as a function of concentration, *p*(c), was calculated as a solution to $p \cdot Q = 0$ according to the following equation:

$$p(\mathrm{c}) = u^{\mathrm{T}} \cdot (S \cdot S^{\mathrm{T}})^{-1}$$

where $S = [Q \quad u]$, and u is a unit column vector. The precise values of the rate constants have no influence on the qualitative behavior we describe here. All mechanisms with these topologies exhibit the same behavior, with only relative occupancies of states varying. (**A**) Equilibrium occupancies are plotted for a mechanism with one binding site for the agonist (A, light blue) and three

conformational changes to open the channel. The state *A-I* (blue, “First Intermediate”) represents receptors that have bound agonist and changed conformation without opening. *A-II* (pink, “Second Intermediate”) represents a further serial conformational change before opening. *AO* (green) is the open state. Occupancy of the resting state (*R,* red) declines monotonically with increasing concentration. No matter how many serial conformational changes are included, the occupancy of each bound state increases monotonically with concentration. (**B**) The same plot for a mechanism with two binding sites for agonist and two conformational changes to open the channel. This model could be considered to represent each dimer in the tetramer, if dimer pairs are assumed to be equivalent. Occupancy of the resting state (*R*) declines monotonically with increasing concentration. Occupancy of each of the fully agonist-bound states (A_2-*R*, A_2-*I* and A_2*O*) increases monotonically. The partially agonist-bound state (*A*-*R*, orange) shows approximately log-normal occupancy, with the maximum close to the EC_{50} for agonist to open the channel. Thus, including multiple binding steps produces at least one state with log-normal occupancy at equilibrium, but multiple conformational changes do not. Given two or more binding sites, any partially agonist-bound state (including any partially agonist-bound open state) will follow this approximately log-normal occupancy. In other words, at equilibrium, the proportion of time spent in the partially agonist-bound state (and therefore the opportunity for trapping) is maximal at an intermediate concentration and vanishingly low at high and low concentrations. Thus, the active fraction (untrapped receptors) follows an inverted bell curve ($1 - P_{A\text{-}R}$). These observations, and the geometric constraints that the LBD subunits A and C must be open for the crosslink at A665C to form, suggest that disulfide trapping occurs preferentially in a partially agonist-bound state.

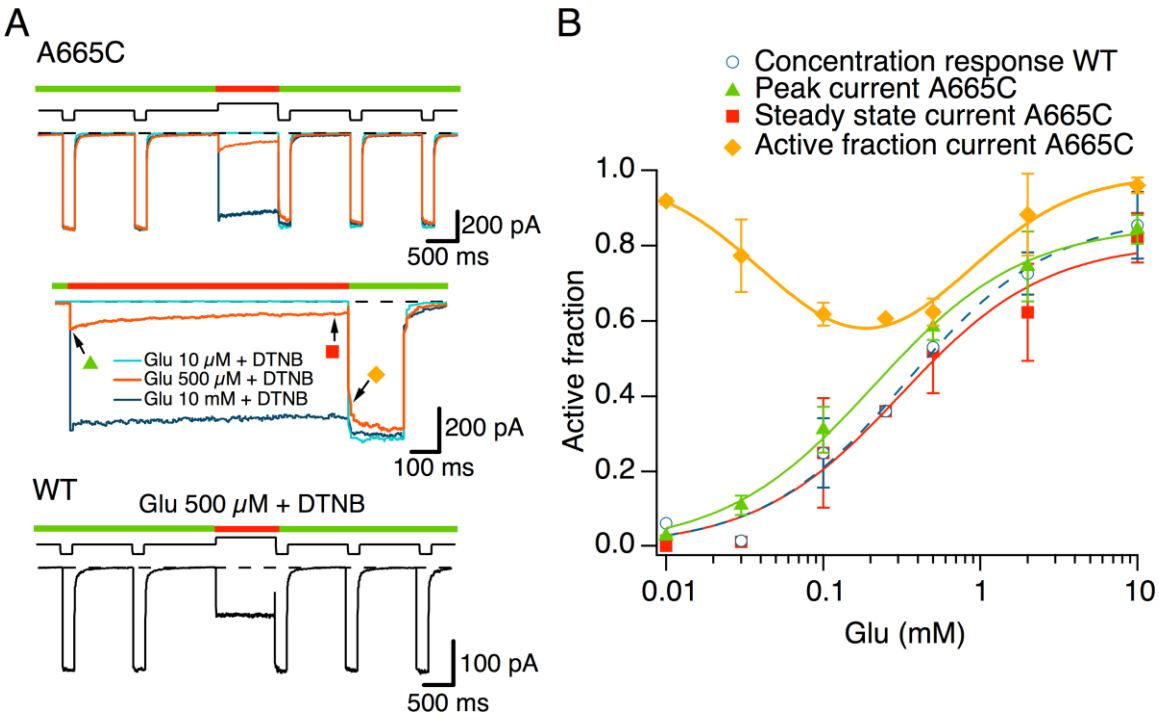

Figure S6. Trapping in the presence of DTNB at different concentrations of glutamate, related to Figure 5. (**A**) In the top panel, three records from the same patch show trapping for glutamate concentrations of 10 µM (light blue trace), 500 µM (orange trace), and 10 mM (dark blue trace) in 500 µM DTNB (red bar). Trapping only occurs in 500 µM glutamate (expanded scale, middle panel). The green bars indicate application of the reducing agent DTE (5 mM). The arrows and symbols indicate the measurements plotted in panel B. Wild-type GluA2 was not modified by 500 µM DTNB with 500 µM glutamate (lower panel, red bar). (**B**) Concentration-response curves in 100 µM CTZ for wild-type GluA2 (blue open circles, EC_{50} = 314 ± 163 µM), GluA2-A665C immediately following reduction with DTE (green triangles; EC_{50} = 400 ± 65 µM), and GluA2-A665C at steady state following trapping in 500 µM DTNB (red squares, EC_{50} = 515 ± 48 µM; P < 0.05 vs. DTE). Plotting the active fraction current after trapping (yellow diamonds) vs. glutamate concentration reveals maximal trapping at 217 µM glutamate (n = 3). All experiments with DTNB also included DTPA (10 µM) in both oxidizing and reducing conditions to chelate trace heavy metals.

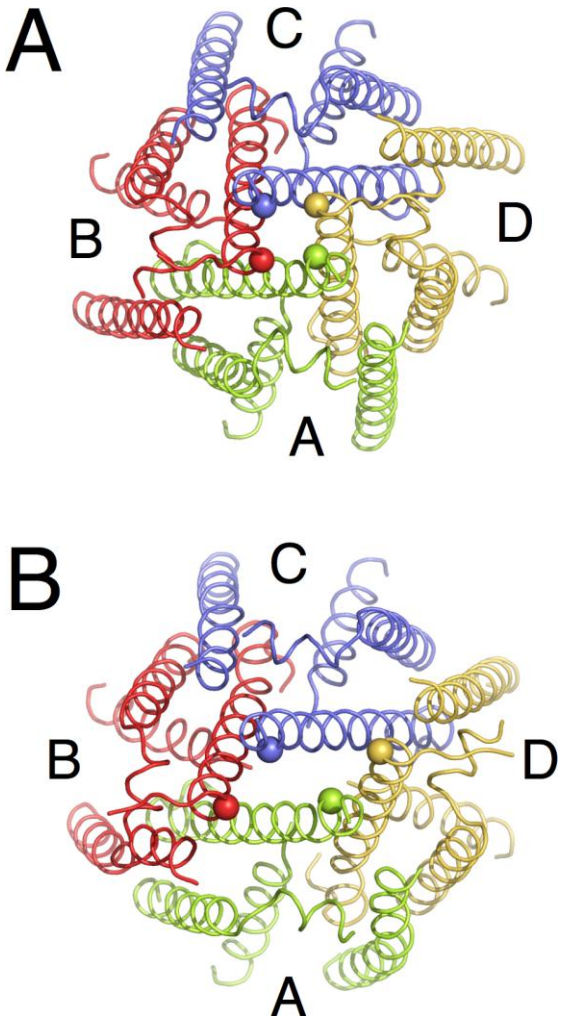

Figure S7. GluA2 ion channel gate conformations, related to Figure 7. (**A**) The conformation observed in the full-length crystal structure (Sobolevsky et al., 2009). T625 Cα atoms, at the gate of the ion channel, are shown as spheres. (**B**) A model generated by adjusting the TMD to fit the crosslinked LBD tetramer CA conformation with the LBDs of subunits B and D modeled in closed conformations (corresponding to tetramer **2** in **Table S1**). The inner transmembrane helices (M3) widen at the ion channel gate between subunits B and D by ~11 Å, as measured between T625.

Tetramer	A–D	B–C	A–B	C–D	A–C	B–D
Pairwise distances between P632 Cα						
1	30.6	30.6	48.9	48.9	35.4	73.4
2	35.1	34.9	51.4	51.9	35.4	80.7
3	17.8	18.3	36.2	36.7	26.6	49.6
4	31.3	30.5	34.1	37.5	29.9	57.7
Pairwise distances between T394 Cα						
1	46.2	46.2	48.9	48.9	84.4	43.8
3	47.2	47.1	65.6	69.4	101.0	55.7

Table S1. Inter-subunit distances (Å), related to Figure 7. In the upper tier, pairwise distances are measured between the P632 Cα atoms of each LBD, which are proximal to the TMD. In the lower tier, pairwise distances are measured between the T394 Cα atoms of each LBD, which are proximal to the ATD. Tetramer **1** is the DNQX-bound crystal structure of the crosslinked LBD tetramer. Tetramer **2** is the crosslinked tetramer with subunits B and D modeled in closed, glutamate-bound conformations. This model was generated by superimposing the crystal structure of a closed, glutamate-bound LBD (PDB ID: 1FTJ (chain A)) (Armstrong and Gouaux, 2000) at helices D and J in Lobe 1. This strategy preserves the back-to-back non-desensitized dimer configuration. Tetramer **3** is the LBD layer from the crystal structure of the antagonist-bound full-length receptor. A comparison of **1** and **3** shows a marked increase in every P632–P632 distance. This increase, however, is due not just to OA-to-CA transitions but also to more open cleft conformations in **3**. Modeled closure of the B and D subunits in the crosslinked tetramer, **2**, unsurprisingly increases all pairwise distances except A-C. The A and C subunits cannot be modeled in closed conformations without breaking the C665–C665 crosslink, consistent with our observation that the crosslink forms when the receptor is not fully occupied by glutamate. Tetramer **4** is similar to **3** but with all subunits modeled in closed conformations. This model was generated as described above for **2**. The closure of all subunits results in an increase in all pairwise distances except A-B.

	A–D	B–C	A–B	C–D	A–C	B–D
OA-to-CA, open LBDs	1.8	1.6	14.0	12.4	9.2	16.8
OA-to-CA, closed LBDs	0.1	1.7	13.2	8.8	2.4	15.5
LBD closure, OA conf.	13.6	12.2	-2.0	0.9	3.4	8.1
LBD closure, CA conf.	11.9	12.3	-2.8	-2.8	-3.4	6.8

Table S2. Modeled inter-LBD distance differences (Å) resulting from either OA-to-CA conformational transitions or LBD closure, related to Figure 7. Distances are measured between the Cα atoms of P632 in each LBD, which are proximal to the TMD. The open LBD conformations correspond to those observed in the crystal structure of the full-length GluA2 receptor (PDB ID: 3KG2) (Sobolevsky et al., 2009). The closed LBD conformation corresponds to the one observed in the crystal structure of a glutamate-bound LBD (PDB ID: 1FTJ (chain A)) (Armstrong and Gouaux, 2000).